Hindawi Publishing Corporation
Journal of Nanoparticles
Volume 2013, Article ID 132180, 10 pages
http://dx.doi.org/10.1155/2013/132180

Research Article

Selective Hydrogenation of *p*-Chloronitrobenzene on Nanosized PdNiB Catalysts

Yu-Wen Chen and Der-Shing Lee

Department of Chemical Engineering, National Central University, Chung-Li 320, Taiwan

Correspondence should be addressed to Yu-Wen Chen; ywchen@ncu.edu.tw

Received 10 January 2013; Accepted 1 February 2013

Academic Editor: Mohammad H. Maneshian

A series of PdNiB bimetallic nanoalloy catalysts with various Pd contents was prepared. Pd was well dispersed in NiB. Even adding a small amount of Pd in NiB had a significant effect on activity and selectivity in hydrogenation of *p*-chloronitrobenzene (*p*-CNB) to *p*-chloroaniline (*p*-CAN). High activity and selectivity on PdNiB could be attributed to both ensemble effect and electronic effect. The particle size in PdNiB decreased with an increase in Pd content. Electron-enriched Ni could activate the polar-NO_2 groups of *p*-CNB and depress the dehalogenation of *p*-CAN.

1. Introduction

Bimetallic nanoparticle catalysts have received increasing attention [1–9]. The most remarkable features of nanoscopic materials are that their chemical and physical properties are quite different from those of bulk solids and those of atoms. This phenomenon has been known as a quantum effect [10–13]. Magnetic enhancement has been expected in Pd clusters owning to their finite size because Pd does not polarize magnetically in bulk metal state, but has giant magnetic moment in the present of ferromagnetic 3d transition metals [14–18]. One could successfully prepare chemically monodispersed ultrafine Pd and bimetallic PdNi particles [17–19].

The addition of the second metal plays a key role in controlling the activity, selectivity, and stability of catalysts in certain reaction. However, little is known about the electronic structures of bimetallic clusters of groups 8–10. Since both Ni and Pd belong to the same group 10 in the periodic table, the increase (mixing) between Ni $3d^8 4s^2$ electrons and Pd $4d^{10} 5s^0$ electrons is very likely involved in intermetallic Ni-Pd bonding [19]. Such effect on the catalysis by nanosized NiPd clusters is certainly interesting.

Aromatic chloramines are important intermediates in the synthesis of dyes, drugs, herbicides, and pesticides [20–34]. At present, these organic amines are generally produced through selective hydrogenation of the corresponding aromatic chloronitro compounds over transition metal catalysts such as Pt and N [35–39]. In this process, the hydrodechlorination of the aromatic chloramines often occurs over most metal catalysts because of the electron-donating effect of amino group in the aromatic ring. Keane [40] reported that in the continuous gas phase hydrogenation of *p*-chloronitrobenzene (*p*-CNB) over several supported Ni catalysts, *p*-chloroaniline (*p*-CAN) was produced as the main product at *p*-CNB conversion of about 15%, which is enlightening for the development of clean route to produce chloroanilines. It has been reported by this lab [41–43] that NiB is more active and selective than Raney nickel catalyst for hydrogenation of *p*-CNB to *p*-CAN. Many modifiers were added on NiB for hydrogenation of chloronitrobenzene [44–70]. Although intensive efforts have been made to solve the problem of hydrodechlorination in CNB hydrogenation, it is still a challenge to create novel catalysts for further improving the selectivity to CAN at complete conversion of the substrates and intermediates and simultaneously maintaining the high catalytic activity [20–32].

Usually the desire selectivity can be achieved by the addition of some inhibitors or some modifiers such as base or other electron-donating compounds to the catalyst or to the solution phase. By alloying a second metal to platinum, Coq

et al. [71, 72] obtained good results in the hydrogenation of *p*-CNB over $PtSn/Al_2O_3$ catalysts, with 97.5% *p*-CAN selectivity at >98% conversion. Comparing with Pt catalysts, Pd catalysts exhibit low selectivity of CAN in the hydrogenation of CNB because the concomitant hydrodechlorination reactions are serious over Pd-based catalysts. The most attractive advantage of Pd-based catalysts over Pt-based ones is its low cost. In order to improve the selectivity to CAN in the hydrogenation of CNB over Pd catalysts, several strategies have been developed, such as introducing some promoting or inhabiting additives to the solution phase or to the catalysts, alloying Pd with other metals, applying partly poisoned catalysts, and modulating the metal/support interaction in supported Pd catalysts. PdB has been reported to be an active catalyst than Pd [14–19].

In a previous paper [9], one of the authors has reported the Pt-NiB catalyst for hydrogenation of *p*-CNB. However, Pt was too active to have high selectivity to the *p*-CAN product. Pd was chosen as the dopant of NiB in this study because its hydrogenation capability was not too high to have high selectivity to *p*-CAN and not too low to have low activity. By adding suitable amount of Pd in NiB, it was expected to have high conversion of *p*-CNB and high selectivity of *p*-CAN.

The objective of this study was to synthesize PdNiB bimetallic nanocatalysts and to investigate the effect of Pd content on the catalytic properties of PdNiB catalysts in liquid-phase hydrogenation of *p*-CNB to *p*-CAN.

2. Experimental

2.1. Materials. *p*-CNB, with a purity of >99%, was obtained from Acros (Belgium). High-purity hydrogen gas (>99.99% from Air Product) was used without further purification. Palladium nitrate and nickel acetate (>98%) were supplied by Showa Chemicals (Tokyo, Japan), and sodium borohydride was purchased from Lancaster (Morecambe, UK). Sodium hydroxide, methanol, and ammonia solutions were purchased from Tedia Co. (OH, USA). Ethanol was purchased from Showa Chemicals (Tokyo, Japan). Raney nickel catalyst was obtained from Merck. All other solvents and reagents were of analytical grade quality, purchased commercially, and used without any further purification. Water used in the whole process was doubly distilled water.

2.2. Catalysts Preparation. A series of PdNiB catalysts was prepared by the chemical reduction method. Pd/Ni atomic ratios were between 0.001 and 0.02 for investigation. Nickel acetate and palladium nitrate were added to the 50% methanol/water solution (both were 0.1 M) at room temperature under vigorous stirring and used nitrogen stream to remove air. The solution of reduction agent, sodium borohydride (1 M), was added with the microtubing pump into the solution drop by drop. The atomic ratio of (Ni + Pd) to B was fixed at 1 : 3. Excess amount of sodium borohydride was used to ensure that all nickel and palladium cations were reduced to metals. When no bubbles were released, the black powders were centrifuged and were washed to remove the impurities, that is, Na^+ ions and the excess amount boride species, by hot deionized water for three times and with methanol twice. Since all catalysts were easily oxidized in air, care must be taken to avoid their exposure to air. Generally, the catalysts were kept in methanol until further use.

2.3. Catalyst Characterization. The catalysts were characterized by XRD, TEM, and XPS. The crystalline structure of the catalysts was characterized by XRD using a Siemens D500 powder X-ray diffractometer. The XRD patterns were collected by using Cu K_α radiation (λ = 0.15418 nm). The tube voltage and current were 40 kV and 40 mA, respectively. The scanning rate was $0.05^\circ\ s^{-1}$.

The morphologies of the catalysts were determined by TEM (Jeol JEM-2000 FX II). TEM was operated at 160 kV and the magnification was 200 K. A small amount of sample was put into the sample tube filled with a 95% ethanol solution. After agitation under ultrasonic environment for 90 min, one drop of the dispersed slurry was dipped onto a carbon coated copper mesh (300#) (Ted Pella Inc., CA, USA) and dried at room temperature in vacuum overnight.

The compositions and the electronic state of each element on the surface of the catalysts were studied by XPS on a Thermo VG Scientific Sigma Probe spectrometer. Al K_α radiation was used as the excitation source ($h\nu$ = 1486.6 eV) (20 kV, 30 mA). The sample was pressed as a self-supported plate and was mounted on the sample cell. It was degassed in the pretreatment chamber at 343 K for 2 h and then it was transferred into the analyzing chamber where the background pressure was lower than 10^{-7} Pa. Before the XPS test, the sample was sputtered using Ar^+ ions for 15 min to remove the oxidation parts, which were formed during the XPS operation. All the binding energies were calibrated by using the contaminant carbon (C1s = 284.6 eV). The XPS spectrum of each element was deconvoluted using a Gaussian-Lorentz curve-fitting program, the background was corrected using a Shirley-type baseline, and the peak type was Gaussian-Lorenz (7 : 3). The surface composition of each sample was calculated using the corresponding peak areas of Ni, Pd, and B, and the PHI sensitive factors were applied in the calculation. It should be noted that, for Ni, only the 2p3/2 subbands were studied instead of the 2p1/2 subbands, because the former have a much higher signal-to-noise ratio and provide the same information.

2.4. Reaction Test. All the experiments were carried out in the cylindrical stirred-tank reactor (Parr Instrument Model 4842). A four-bladed pitched impeller was placed for effective agitation, and the agitator was connected to an electric motor with variable speed up to 1700 rpm. A pressure transmitter and an automatic temperature controller were also provided. Hydrogen was introduced at the bottom of the reactor. A separate tube was used as sampling tube for the liquid phase. The reactor was charged by 0.002 mol Ni catalyst and 2.54 g *p*-CNB in 80 mL methanol; the concentration of *p*-CNB was 0.2 M. It was reported that methanol was a better reaction medium than ethanol for the hydrogenation reaction. The reaction was operated in reaction-controlled regime, as confirmed by using the different particle size and

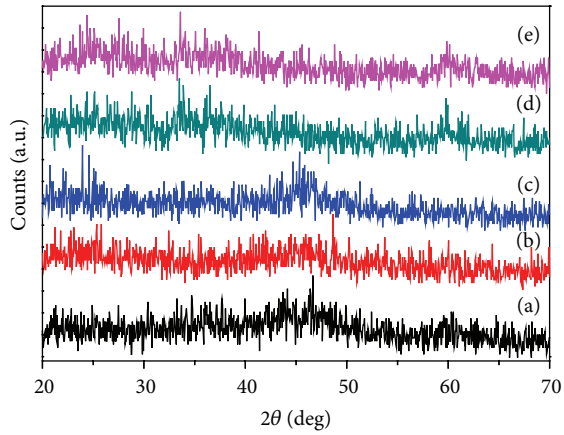

Figure 1: XRD patterns of catalyst samples, (a) NiB, (b) 0.001Pd-NiB, (c) 0.005Pd-NiB, (d) 0.01Pd-NiB, and (e) 0.02Pd-NiB.

stirring rate. The results showed that 400 rpm was enough to free from external diffusion. Therefore, 500 rpm stirring speed was used in this study. PdNiB sample was in nanosize range; one can conclude that the pore diffusion was not important in this study. During the reaction run, the samples were withdrawn periodically (every 10 min) and analyzed by a gas chromatograph equipped with a flame ionization detector and a 3 m × 1/8 inch stainless steel column packed with 5% OV-101 on Chromosorb WAW-DMSC (80–100 mesh). The conversion and the selectivity of each product were calculated as follows:

$$\begin{aligned}
&\text{conversion (\%)} \\
&= \left(1 - \frac{C_{p\text{-CNB}}}{C_{\text{AN}} + C_{\text{NB}} + C_{p\text{-CAN}} + C_{p\text{-CNB}}}\right) \times 100\%, \\
S_{\text{AN}}\,(\%) &= \left(\frac{C_{\text{AN}}}{C_{\text{AN}} + C_{\text{NB}} + C_{p\text{-CAN}}}\right) \times 100\%, \\
S_{\text{NB}}\,(\%) &= \left(\frac{C_{\text{NB}}}{C_{\text{AN}} + C_{\text{NB}} + C_{p\text{-CAN}}}\right) \times 100\%, \\
S_{p\text{–CAN}}\,(\%) &= \left(\frac{C_{p\text{-CAN}}}{C_{\text{AN}} + C_{\text{NB}} + C_{p\text{-CAN}}}\right) \times 100\%,
\end{aligned} \tag{1}$$

where C_{AN}, C_{NB}, $C_{p\text{-CAN}}$, and $C_{p\text{-CNB}}$ represented the concentration of aniline, nitrobenzene, *p*-chloroaniline, and *p*-chloronitrobenzene, respectively.

3. Results and Discussion

3.1. XRD. XRD was used to characterize the structure of the Pd-NiB bimetallic nanoparticles. The XRD patterns of NiB and Pd-NiB samples with various contents of Pd are shown in Figure 1. The broad peak at $2\theta = 45^\circ$ in each pattern indicates the amorphous phase in all the as-prepared samples, in consistent with those in the literature [9, 11, 12]. It is further evidenced by a diffuse Debye ring rather than distinct dots in their SAED patterns. It has been reported that Ni can form several types of compounds with B such as NiB, Ni_2B, and Ni_3B. After adding the Pd, the intensities of this peak decreased. This shows that the presence of Pd could suppress the crystalline growth (long-range order) of NiB. No diffraction peak corresponding to crystalline Pd was found, indicating a high dispersion of Pd in NiB. No other crystalline phases (including palladium-related compounds, elemental Ni, B, and the corresponding oxides and hydroxides) were observed. One can conclude that PdNiB possessed short-range order and long range disorder, resulting in more surface coordinating unsaturated sites, more crystalline defects, and isotropic structure. Alloying Pd interrupts the long-range order of NiB, resulting in the characteristics of small cluster of NiB. Wang et al. [73] reported that a metal can disperse on the surface of another metal to form a highly dispersed bimetallic system due to the formation of bonds between the two metals. They noted that a highly dispersed Pd-Ni system occurred when <2.0 wt% Pd was loaded on a Pd/Ni catalyst. Our results are in accord.

3.2. TEM. Figure 2 shows the morphology of the as-prepared samples. With the addition of Pd, the particle size tends to decrease. Due to the high surface energy of the nanosized amorphous alloys, metal metalloids prepared by chemical reduction with borohydride are inclined to aggregate to form larger particles with diameters of several 10s to several 100s nanometers. Each sample was composed of many small particles, and the size of the aggregates was about 50 nm. It was difficult to obtain detailed information on the TEM photos because of the aggregation of the particles by the very strong van der Waals force and magnetization. One was not able to see any Pd particles due to very low concentration in the sample. After adding Pd on NiB, it became difficult to sediment in water, indicating that Pd-NiB particles were smaller than NiB particles. The primary particles of PdNiB were very fine. One could conclude that the size of primary particles of PdNiB was much smaller than 50 nm. Moreover, the magnetization of ultrafine particles remarkably increased with doping Pd into NiB.

3.3. XPS. The compositions and the electronic structure of each species on the surface of the samples were determined by XPS analysis. All of the spectra were deconvoluted, and the amount of each species in each state was calculated based on the corresponding peak area. The XPS spectra of Ni_{2p} and B_{1s} are shown in Figures 3 and 4. The binding energy of Ni_{2p} level is ascribed to 856.8, 857.7, 856.0, 853.4, 856.3, and 856.7 eV, respectively, for the samples of NiB, 0.001Pd-NiB, 0.005Ni-PdB, 0.01Pd-NiB, and 0.02Pd-NiB. These are assigned to the metallic nickel. The peak around 862.2 eV is ascribed to nickel oxide (it was simply donated as Ni^{2+} for the oxidized state of Ni; similar notations were used for the other elements). Tolman et al. [74] investigated a variety of Ni^0 organometallic compounds and found that in zero-valence state Ni complexes, the $Ni_{2p3/2}$ binding energies span a range of 853.6–856.0 eV, while higher binding energy peaks were observed in a range of 855.0–857.2 eV in Ni^{2+} complexes, and even higher

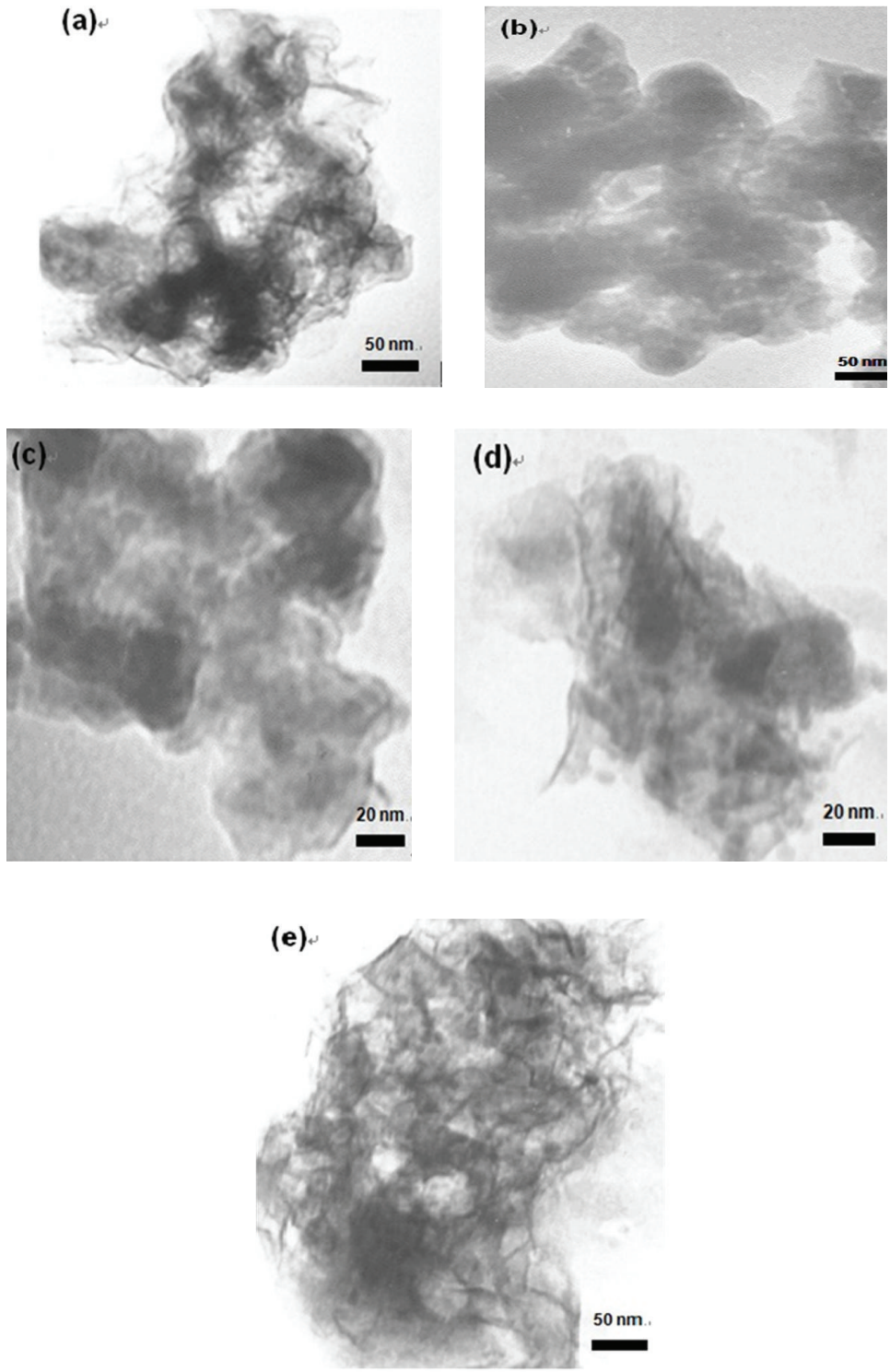

Figure 2: TEM images of (a) NiB, (b) 0.001Pd-NiB, (c) 0.005Pd-NiB, (d) 0.01Pd-NiB, and (e) 0.02Pd-NiB.

binding energy peaks were observed for Ni^{4+} compounds [74]. Matienzo et al. [75] also extensively studied a series of nickel compounds in all of the oxidation states by XPS. In NiO, binding energy values of 854.0 and 872.0 eV were found for $Ni_{2p3/2}$ and $Ni_{2p1/2}$ peaks, respectively. Furthermore, in the case of NiO and tetrahedral Ni^{2+} compounds, obvious shake-up (satellite) peaks can be found in the region at about 6 eV higher than a normal $Ni_{2p3/2}$ or $Ni_{2p1/2}$ band because such compounds are paramagnetic, whereas Ni^0 compounds and square-planar complexes of Ni^{2+} do not produce satellite

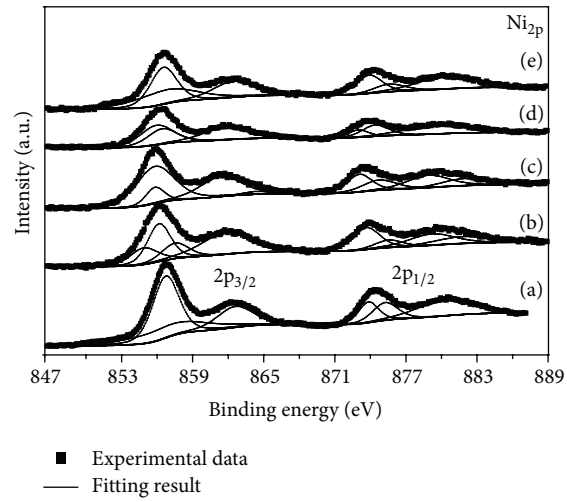

Figure 3: XPS spectra of Ni_{2p} for (a) NiB, (b) 0.001Pd-NiB, (c) 0.005Pd-NiB, (d) 0.01Pd-NiB, and (e) 0.02Pd-NiB.

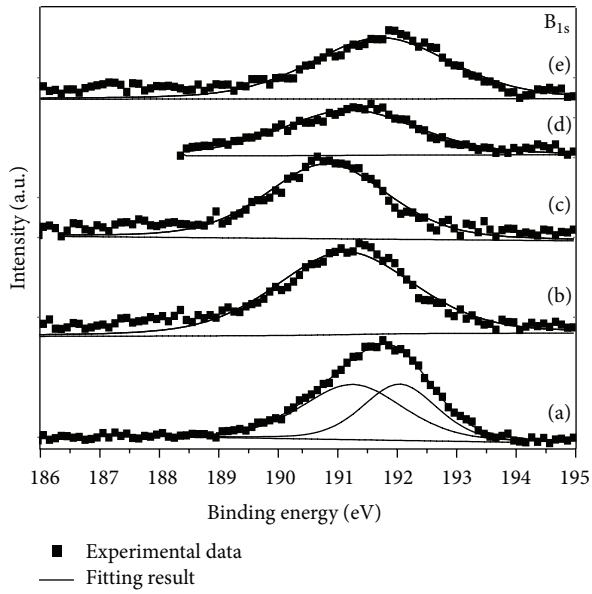

Figure 4: XPS spectra of B_{1s} for (a) NiB, (b) 0.001Pd-NiB, (c) 0.005Pd-NiB, (d) 0.01Pd-NiB, and (e) 0.02Pd-NiB.

peaks, because they are diamagnetic. Therefore, the Ni_{2p} bands in Figure 3 show low binding energy values and essentially no satellites features inferring that Ni exists mainly as zero-valence state inside PdNiB rather than in NiO-Pd-B form. The PdNiB catalysts exhibited electron-enriched state and effectively dispersed the Ni nanoparticles, resulting in more metallic Ni atoms on the surface. It is consistent with the results in the literature [76]. No obvious shift was presented in the XPS spectra, and those present in metallic state are not very close to the standard value 853.1 eV [77], which was attributed to the quantum size effect. It is known that hydrogen molecules adsorbed on the Ni^0 sites are activated to proceed hydrogenation reaction. Therefore, the amount of Ni^0 on the surface of catalyst is crucial for its catalytic activity in hydrogenation reaction.

There are two peaks in the B_{1s} spectra. The peak near 187.1 eV is attributed to elemental B, and the peak near 192.5 eV is attributed to B^{3+}. The peak with the binding energy around 192.5 eV is related to the presence of the oxidized B species, which may be attributed to the interaction between BH_4^- and H_2O during the reduction of Pd^{2+} ions by BH_4^- in alkali solution or the surface boron oxide in the Pd-NiB alloy oxidized by air. It should be noted that most of B species is in oxidation state. The binding energies of B_{1s} are 191.6, 191.2, 190.9, 191.2, and 191.8 eV for the samples of NiB, 0.001PdNiB, 0.005PdNiB, 0.01PdNiB, and 0.02PdNiB, respectively. The decreased BE's resulted from acceptance of electrons of B from other metal atoms. Strong interaction and interdiffusion between Pd and B substrate at room temperature have been reported [18, 78]. Here the change in BE's should be due to the interaction of Ni, Pd, and B. In conclusion, the amorphous structure of NiB and the presence of B promoted the surface-alloying effect of Pd and Ni. Pd peak was not observed due to the low loadings in these samples.

3.4. Hydrogenation Reaction. The catalytic activities of the as-prepared catalysts were investigated on the hydrogenation of *p*-CNB. There are two kinds of reactions in the hydrogenation process: selected hydrogenation of $-NO_2$ group and dehalogenation of –Cl group. In order to obtain high *p*-CAN yield, the dechlorination of *p*-CNB and *p*-CAN should be restrained; only the hydrogenation of $-NO_2$ group of *p*-CNB is desired [79]. The simplified reaction route is displayed in Scheme 1.

Figure 5 shows the conversion of *p*-CNB and the corresponding selectivity of *p*-CAN over these catalysts. The yields of *p*-CAN, NB, and AN are also shown in Figure 5. In each case, the concentration of NB increased at the first 30 min and then decreased and converted to AN and became zero eventually. There are two possible explanations the other one is that *p*-CNB only followed path (1) in reaction scheme in the first 30 min; is that the rate of the hydrogenation on the path (3) is faster than path (1). Since the increasing rate of aniline is not obvious, so the possibility of the latter case is low.

Figure 5 shows the *p*-CNB conversion and the selectivity of *p*-CAN versus reaction time. The reaction rate was zeroth order to *p*-CNB concentration. The activity of PdNiB was greater than NiB even with very small amount of Pd. The reaction results of the catalysts are listed in Table 1. The sample 0.02Pd-NiB had the highest reaction rate, which achieved 100% conversion within 30 min. The results showed that the activities increased with an increase in Pd content in the range of Pd/Ni atomic ratios between 0 and 0.01. Even adding small amount of Pd could enhance the activity and selectivity of *p*-CAN greatly. The hydrogenation of *p*-CNB on PdNiB catalysts was very selective to *p*-CAN. The results demonstrated that PdNiB can have the advantages of both metals, that is, high activity of Pd and high selectivity of Ni.

Both Ni^0 and Pd^0 are the active sites. Since only very small amount of Pd was added, the reaction was mainly on the surface of Ni. The surface concentration and electron

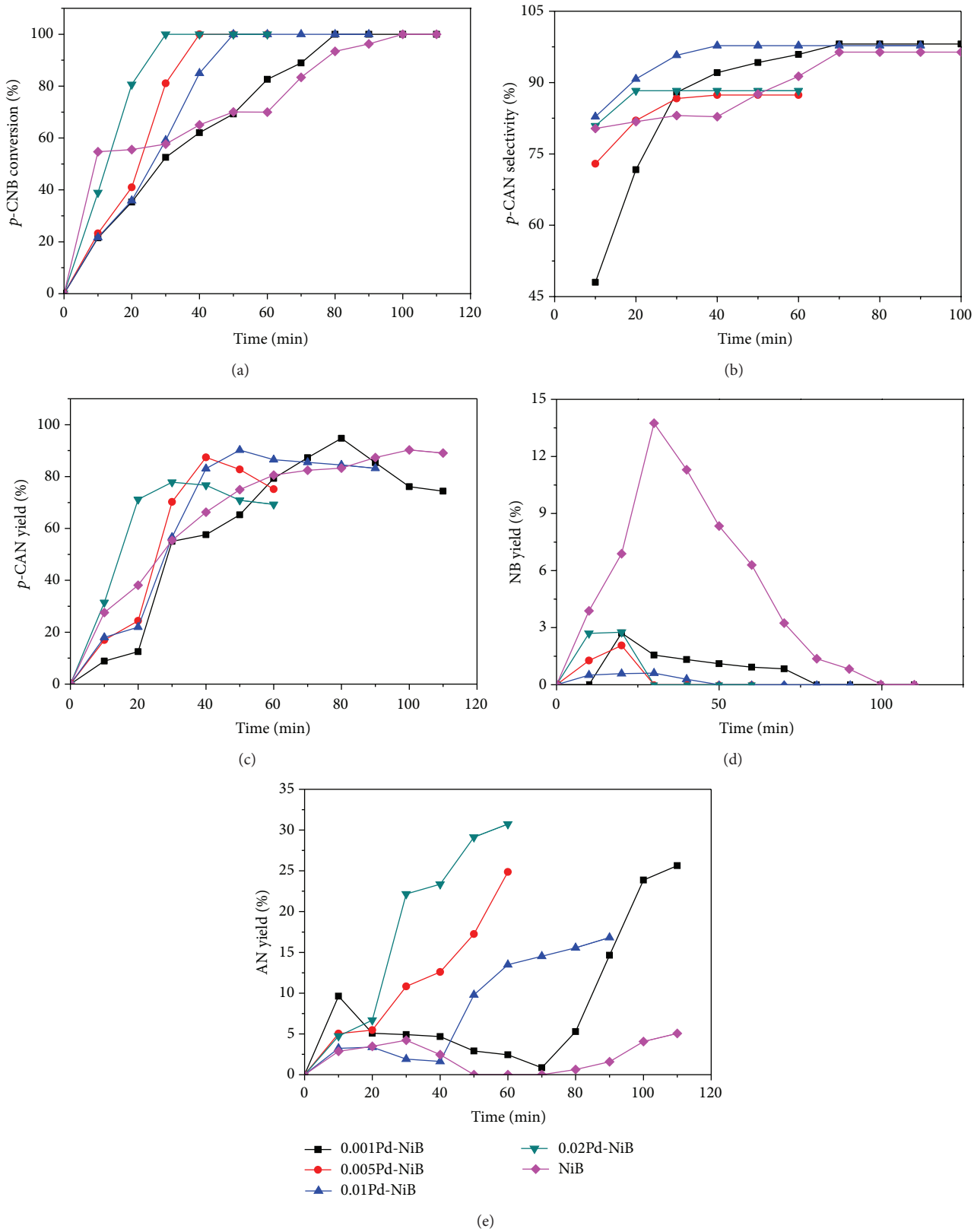

Figure 5: The relations of (a) *p*-CNB conversion, (b) *p*-CAN selectivity, (c) *p*-CAN yield, (d) NB yield, and (e) AN yield with reaction time on PdNiB catalysts. *Reaction conditions: 2 mmol NiPdB catalyst; 16 mmol *p*-CNB; 80 mL methanol; 80°C; 1.2 MPa hydrogen pressure; 500 rpm.

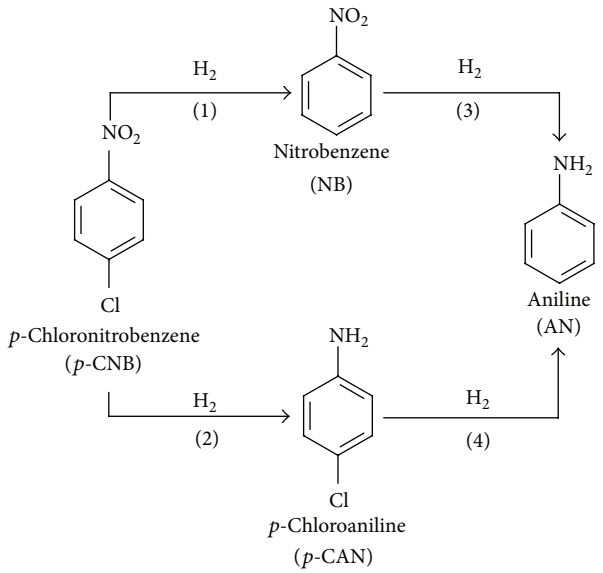

Scheme 1: Simplified reaction scheme of hydrogenation of *p*-CNB.

density of Ni^0 are the important factors for the reaction. A higher Ni^0 content would favor the dissociative adsorption of H_2 molecules. According to the XPS analysis, one could find out that all the prepared samples had high densities of the elemental Ni. Thus, the $-NO_2$ group in the reactant *p*-CNB can be activated by the positive-charged Pd. The ability of the nearby dissociated H atoms to attack the O and N atoms of $-NO_2$ groups to form $-NH_2$ is enhanced, which benefits the high selectivity of *p*-CAN [33, 35, 80]. With the addition of Pd, the binding energy of Ni shifted to a lower value, indicating that Ni received more electrons from Pd. Combining the structure effect, palladium species could make the Ni particles smaller. This would increase the dispersion of Ni active sites and make the surface of the catalyst highly unsaturated, which favors the hydrogenation of *p*-CNB. The nitro group owned two different elements, N and O; both are highly electronegative. With the electrons donation from alloying B and Pd to Ni, the Ni on the catalyst surface became more electron enriched. Higher electronegativity of $-NO_2$ would be adsorbed on the surface easily, and the active sites would activate the N=O bond, which was polarized. The para-substituted nitro group had the higher electron negativity, resulting from the combination of both inductive and resonance effects. Since the $-NO_2$ group was more electronegative than –Cl, $-NO_2$ was supposed to occupy the active site on Ni surface at the start of the reaction. $-NO_2$ adsorbed on the catalyst surface is hydrogenated to form *p*-CAN, which is further desorbed. In addition, oxygen was more electronegative and alloying Pd and B could engage the oxygen to activate the polar $-NO_2$ group of *p*-CNB. The $-NH_2$ of *p*-CAN might adsorb on the surface alloying B and Pd and coordinate with each other. It would improve the selectivity of *p*-CAN by depressing the dehalogenation reaction. Pd-dopant in the NiB catalysts would increase the electron density of Ni and make the activity increase significantly. In addition, PdNiB is paramagnetic; it is easier to separate after reaction.

Table 1: The Effect of Pd content on the hydrogenation of *p*-CNB over PdNiB catalysts[a].

Sample	Reaction time (min) to 100% conversion[a]	Selectivity (%)			Reaction rate constant (s^{-1})
		p-CAN[b]	AN[b]	NB[b]	
NiB	95.6	96.9	5.5	0	0.0298
0.001Pd-NiB	80.0	94.7	5.3	0	0.0167
0.005Pd-NiB	40.0	75.1	24.9	0	0.0119
0.01Pd-NiB	50.0	90.2	9.8	0	0.0127
0.02Pd-NiB	28.6	77.8	22.2	0	0.0112

[a]Reaction condition: 1.2 MPa hydrogen pressure, 353 K reaction temperature, absolute methanol was medium, 500 rpm stirring speed, and 0.2 mmol Ni catalyst.
[b]*p*-CAN: *p*-chloroaniline; AN: aniline; NB: nitrobenzene.

The results presented herein show that metal catalyst could be affected by the formation of the bimetallic colloid or by the addition of metal cations. The mechanism of the hydrogenation of *p*-CNB over the bimetallic collided system is very complicate and is affected by the electronic and conformation properties of the components as well as the composition on the mental surface.

3.5. Reaction Kinetics. One could calculate the reaction rate constant for each catalyst. Based on the conversion-time curves in the hydrogenation of *p*-CNB (Figure 5), it shows that the reaction was of first order with respect to the concentration of *p*-CNB [81]. The reaction rate can be expressed as

$$-r_A = kC_{A0} \cdot (1 - X_A), \tag{2}$$

where k is the reaction rate constant, s^{-1}; C_{A0} is the the initial concentration of reactant at $t = 0$; X_A is the conversion of A.

Since the reaction was carried out in a constant-volume batch reactor, so

$$-r_A = C_{A0}\frac{dX_A}{dt}, \tag{3}$$

where C_{A0} is the the initial concentration of reactant at $t = 0$; X_A is the conversion of A; t is the reaction time.

Combining the above two equations and using integral method of analysis of data, one could get

$$-\ln(1 - X_A) = kt. \tag{4}$$

A plot of $-\ln(1 - X_A)$ versus t could derive the slope which represents the reaction rate constant. Because of the induction period appeared in the initial stage of reaction, the data in the initial stage were neglected. The results are tabulated in Table 1. As expected, the rate constant of NiPdB catalyst was higher than that of NiB.

4. Conclusion

A series of PdNiB nanoalloy catalysts with various Pd contents was prepared by chemical reduction method with

$NaBH_4$ as the reducing agent. The catalysts were characterized by XRD, TEM, and XPS. The catalytic properties of these catalysts were tested in the hydrogenation of *p*-CNB. NiB was amorphous as indicated by the broad peak around $2\theta = 45^\circ$. Upon modification with Pd, it could maintain NiB in the amorphous structure and decrease the crystallinity. With the addition of Pd, the particle size of NiB decreased. PdNiB formed nanoalloy and no discrete phase was found. The addition of Pd could reduce the particle size of NiB and improve the Ni dispersion. The binding energy of elemental Ni and B in the PdNiB is negatively shifted, indicating that Ni and B accepted partial electrons from Pd. The magnetization of PdNiB remarkably increased with doping Pd into NiB.

Since the $-NO_2$ was more electronegative than –Cl, $-NO_2$ was supposed to occupy the active site on Ni surface in the beginning of the reaction. $-NO_2$ adsorbed on the surface is hydrogenated to form *p*-CAN which is then desorbed. In addition, oxygen is more electronegative and the alloying B could engage the oxygen to activate the polar $-NO_2$ group of *p*-CNB. The $-NH_2$ of *p*-CAN might adsorb on the alloying B and coordinate with each other. Hence, it could improve the selectivity of *p*-CAN by suppressing the dehalogenation reaction.

High activity and selectivity on PdNiB in the hydrogenation of *p*-CNB could be attributed to both ensemble effect and electronic effect. Alloying Pd interrupts the long-range order of NiB, resulting in the characteristics of small cluster of NiB. On the other hand, B and Pd could partially donate electrons to Ni. Electron-enriched Ni could activate the polar $-NO_2$ groups of *p*-CNB and depress the dehalogenation of *p*-CAN. The results described here showed that PdNiB nanoalloy catalyst is a promising catalyst for industrial application.

Acknowledgment

This research was supported by the Ministry of Economical Affairs, Taiwan, under Contract no. 101-EC-17-A-09-S1- 022.

References

[1] J. Q. Du, Y. Zhang, T. Tian, S. C. Yan, and H. T. Wang, "Microwave irradiation assisted rapid synthesis of Fe–Ru bimetallic nanoparticles and their catalytic properties in water-gas shift reaction," *Materials Research Bulletin*, vol. 44, no. 6, pp. 1347–1351, 2009.

[2] J. C. S. Wu and H. C. Chou, "Bimetallic Rh–Ni/BN catalyst for methane reforming with CO_2," *Chemical Engineering Journal*, vol. 148, no. 2-3, pp. 539–545, 2009.

[3] N. He, P. Li, Y. Zhou, W. Ren, S. Fan, and V. A. Verkhozina, "Catalytic dechlorination of polychlorinated biphenyls in soil by palladium-iron bimetallic catalyst," *Journal of Hazardous Materials*, vol. 164, no. 1, pp. 126–132, 2009.

[4] G. Bernardotto, F. Menegazzo, F. Pinna, M. Signoretto, G. Cruciani, and G. Strukul, "New Pd–Pt and Pd–Au catalysts for an efficient synthesis of H_2O_2 from H_2 and O_2 under very mild conditions," *Applied Catalysis A*, vol. 358, no. 2, pp. 129–135, 2009.

[5] S. Penner, H. Lorenz, W. Jochum et al., "Pd/Ga_2O_3 methanol steam reforming catalysts, part I: morphology, composition and structural aspects," *Applied Catalysis A*, vol. 358, no. 2, pp. 193–202, 2009.

[6] N. M. Bertero, A. F. Trasarti, B. Moraweck, A. Borgna, and A. J. Marchi, "Selective liquid-phase hydrogenation of citral over supported bimetallic Pt–Co catalysts," *Applied Catalysis A*, vol. 358, no. 1, pp. 32–41, 2009.

[7] M. P. Latusek, R. M. Heimerl, B. P. Spigarelli, and J. H. Holles, "Synthesis and characterization of supported bimetallic overlayer catalysts," *Applied Catalysis A*, vol. 358, no. 1, pp. 79–87, 2009.

[8] N. Gyorffy, I. Bakos, S. Szabo et al., "Preparation, characterization and catalytic testing of GePt catalysts," *Journal of Catalysis*, vol. 263, no. 2, pp. 372–379, 2009.

[9] Y. W. Chen, N. Sasirekha, and Y. C. Liu, "Hydrogenation of *p*-chloronitrobenzene over NiPtB nanoalloy catalysts," *Journal of Non-Crystalline Solids*, vol. 355, no. 22-23, pp. 1193–1201, 2009.

[10] G. C. Bond and D. E. Webster, "Mixed metal catalysts in catalytic hydrogenation," *Annals of the New York Academy of Sciences*, vol. 158, pp. 540–559, 1969.

[11] L. F. Chen and Y. W. Chen, "Effect of additive (W, Mo, and Ru) on Ni–B amorphous alloy catalyst in hydrogenation of *p*-chloronitrobenzene," *Industrial & Engineering Chemistry Research*, vol. 45, no. 26, pp. 8866–8873, 2006.

[12] Y. Chen, "Chemical preparation and characterization of metal-metalloid ultrafine amorphous alloy particles," *Catalysis Today*, vol. 44, no. 1–4, pp. 3–16, 1998.

[13] X. F. Chen, H. X. Li, H. S. Luo, and M. H. Qiao, "Liquid phase hydrogenation of furfural to furfuryl alcohol over Mo-doped Co-B amorphous alloy catalysts," *Applied Catalysis A*, vol. 233, no. 1-2, pp. 13–20, 2002.

[14] T. Ding, Y. N. Qin, and M. A. Zhi, "Study of the Pd-B/γ-Al_2O_3 amorphous alloy catalyst," *Chinese Chemical Letters*, vol. 14, no. 3, pp. 319–322, 2003.

[15] X. Yu, M. Wang, and H. Li, "Study on the nitrobenzene hydrogenation over a Pd-B/SiO_2 amorphous catalyst," *Applied Catalysis A*, vol. 202, no. 1, pp. 17–22, 2000.

[16] W. X. Tu, S. J. Cao, L. P. Yang, and W. C. Wang, "Modification effects of magnetic supports and bimetallic structures on palladium nanocluster catalysts," *Chemical Engineering Journal*, vol. 143, no. 1–3, pp. 244–248, 2008.

[17] F. J. Urbano and J. M. Marinas, "Hydrogenolysis of organohalogen compounds over palladium supported catalysts," *Journal of Molecular Catalysis A*, vol. 173, no. 1-2, pp. 329–345, 2001.

[18] D. H. Shen, P. A. Kearney, J. M. Slaughter, and C. M. Falco, "Chemical interaction at the Pd-B interface," *Journal of Magnetism and Magnetic Materials*, vol. 126, no. 1–3, pp. 25–27, 1993.

[19] S. U. Son, Y. Jang, J. Park et al., "Designed synthesis of atom-economical Pd/Ni bimetallic nanoparticle-based catalysts for sonogashira coupling reactions," *Journal of the American Chemical Society*, vol. 126, no. 16, pp. 5026–5027, 2004.

[20] B. Coq, G. Ferrat, and F. Figueras, "Conversion of chlorobenzene over palladium and rhodium catalysts of widely varying dispersion," *Journal of Catalysis*, vol. 101, no. 2, pp. 434–445, 1986.

[21] B. Coq, A. Tijani, and F. Figuéras, "Hydrogenation of *para*-chloronitrobenzene over supported ruthenium-based catalysts," *Applied Catalysis*, vol. 76, no. 2, pp. 255–266, 1991.

[22] N. Lingaiah, N. S. Babu, R. Gopinath, P. S. S. Reddy, and P. S. S. Prasad, "Hydrodechlorination of chlorobenzene over supported metal catalysts," *Catalysis Surveys from Asia*, vol. 10, no. 1, pp. 29–39, 2006.

[23] L. M. Sikhwivhilu, N. J. Coville, B. M. Pulimaddi, J. Venkatreddy, and V. Vishwanathan, "Selective hydrogenation of *o*-chloronitrobenzene over palladium supported nanotubular titanium dioxide derived catalysts," *Catalysis Communications*, vol. 8, no. 12, pp. 1999–2006, 2007.

[24] M. Liu, W. Yu, H. Liu, and J. Zheng, "Preparation and characterization of polymer-stabilized ruthenium–platinum and ruthenium–palladium bimetallic colloids and their catalytic properties for hydrogenation of *o*-chloronitrobenzene," *Journal of Colloid and Interface Science*, vol. 214, no. 2, pp. 231–237, 1999.

[25] M. H. Liu, W. Y. Yu, and H. F. Liu, "Selective hydrogenation of *o*-chloronitrobenzene over polymer-stabilized ruthenium colloidal catalysts," *Journal of Molecular Catalysis A*, vol. 138, no. 2-3, pp. 295–303, 1999.

[26] Y. W. Chen and D. S. Lee, "Hydrogenation of *p*-chloronitrobenzene on nanosized modified NiMoB catalysts," *Catalysis Survey in Asia*, vol. 16, pp. 198–209, 2012.

[27] Y. Monguchi, A. Kume, K. Hattori, T. Maegawa, and H. Sajiki, "Pd/C–Et_3N-mediated catalytic hydrodechlorination of aromatic chlorides under mild conditions," *Tetrahedron*, vol. 62, no. 33, pp. 7926–7933, 2006.

[28] V. Vishwanathan, V. Jayasri, P. M. Basha, N. Mahata, L. Sikhwivhilu, and N. J. Coville, "Gas phase hydrogenation of *ortho*-chloronitrobenzene (O-CNB) to *ortho*-chloroaniline (O-CAN) over unpromoted and alkali metal promoted-alumina supported palladium catalysts," *Catalysis Communications*, vol. 9, no. 3, pp. 453–458, 2008.

[29] C. Y. Xi, H. Y. Cheng, J. M. Hao, S. X. Cai, and F. Y. Zhao, "Hydrogenation of *o*-chloronitrobenzene to *o*-chloroaniline over Pd/C in supercritical carbon dioxide," *Journal of Molecular Catalysis A*, vol. 282, no. 1-2, pp. 80–84, 2008.

[30] X. L. Yang, H. F. Liu, and H. Zhong, "Hydrogenation of *o*-chloronitrobenzene over polymer-stabilized palladium–platinum bimetallic colloidal clusters," *Journal of Molecular Catalysis A*, vol. 147, no. 1-2, pp. 55–62, 1999.

[31] Z. K. Yu, S. J. Liao, Y. Xu, B. Yang, and R. Yu, "A remarkable synergic effect of polymer-anchored bimetallic palladium–ruthenium catalysts in the selective hydrogenation of *p*-chloronitrobenzene," *Journal of the Chemical Society, Chemical Communications*, no. 11, pp. 1155–1156, 1995.

[32] Z. K. Yu, S. J. Liao, Y. Xu, B. Yang, and D. R. Yu, "Hydrogenation of nitroaromatics by polymer-anchored bimetallic palladium–ruthenium and palladium–platinum catalysts under mild conditions," *Journal of Molecular Catalysis A*, vol. 120, no. 1–3, pp. 247–255, 1997.

[33] X. X. Han, R. X. Zhou, G. H. Lai, B. H. Yue, and X. M. Zheng, "Effect of transition metal (Cr, Mn, Fe, Co, Ni and Cu) on the hydrogenation properties of chloronitrobenzene over Pt/TiO_2 catalysts," *Journal of Molecular Catalysis A*, vol. 209, no. 1-2, pp. 83–87, 2004.

[34] J. R. Kosak, "Catalytic hydrogenation of aromatic halonitro compounds," *Annals of the New York Academy of Sciences*, vol. 172, pp. 175–185, 1970.

[35] H. Li, Q. F. Zhao, and H. X. Li, "Selective hydrogenation of *p*-chloronitrobenzene over Ni–P–B amorphous catalyst and synergistic promoting effects of B and P ," *Journal of Molecular Catalysis A*, vol. 285, no. 1-2, pp. 29–35, 2008.

[36] N. Mahata, A. F. Cunha, J. J. M. Órfão, and J. L. Figueiredo, "Hydrogenation of chloronitrobenzenes over filamentous carbon stabilized nickel nanoparticles," *Catalysis Communications*, vol. 10, no. 8, pp. 1203–1206, 2009.

[37] M. H. Lin, B. Zhao, and Y. W. Chen, "Hydrogenation of *p*-chloronitrobenzene over Mo-modified NiCoB nanoalloy catalysts: effect of Mo content," *Industrial & Engineering Chemistry Research*, vol. 48, no. 15, pp. 7037–7043, 2009.

[38] B. Zhao, C. J. Chou, and Y. W. Chen, "Hydrogenation of *p*-chloronitrobenzene on tungsten-modified NiCoB catalyst," *Industrial & Engineering Chemistry Research*, vol. 49, no. 4, pp. 1669–1676, 2010.

[39] B. Zhao and Y. W. Chen, "Hydrogenation of *p*-chloronitrobenzene on Mo, La, Fe, and W-modified NiCoB nanoalloy catalysts," *Journal of Non-Crystalline Solids*, vol. 356, no. 18-19, pp. 839–847, 2010.

[40] M. A. Keane, "A review of catalytic approaches to waste minimization: case study-liquid-phase catalytic treatment of chlorophenols," *Journal of Chemical Technology and Biotechnology*, vol. 80, no. 11, pp. 1211–1222, 2005.

[41] Y. C. Liu, C. Y. Huang, and Y. W. Chen, "Hydrogenation of *p*-chloronitrobenzene on Ni–B nanometal catalysts," *Journal of Nanoparticle Research*, vol. 8, no. 2, pp. 223–234, 2006.

[42] Y. C. Liu, C. Y. Huang, and Y. W. Chen, "Liquid-phase selective hydrogenation of *p*-chloronitrobenzene on Ni–P–B nanocatalysts," *Industrial & Engineering Chemistry Research*, vol. 45, no. 1, pp. 62–69, 2006.

[43] Y. C. Liu and Y. W. Chen, "Hydrogenation of *p*-chloronitrobenzene on lanthanum-promoted NiB nanometal catalysts," *Industrial & Engineering Chemistry Research*, vol. 45, no. 9, pp. 2973–2980, 2006.

[44] J. F. Deng, J. Yang, S. Sheng, and H. Chen, "The study of ultrafine Ni–B and Ni–P amorphous alloy powders as catalysts," *Journal of Catalysis*, vol. 150, no. 2, pp. 434–438, 1994.

[45] J. F. Deng, H. Li, and W. J. Wang, "Progress in design of new amorphous alloy catalysts," *Catalysis Today*, vol. 51, no. 1, pp. 113–125, 1999.

[46] S. P. Lee and Y. W. Chen, "Nitrobenzene hydrogenation on Ni–P, Ni–B and Ni–P–B ultrafine materials," *Journal of Molecular Catalysis A*, vol. 152, no. 1-2, pp. 213–223, 2000.

[47] C. P. Li, Y. W. Chen, and W. J. Wang, "Nitrobenzene hydrogenation over aluminum borate-supported platinum catalyst," *Applied Catalysis A*, vol. 119, no. 2, pp. 185–194, 1994.

[48] H. Li, H. X. Li, W. L. Dai, W. J. Wang, and Z. G. Fang, "XPS studies on surface electronic characteristics of Ni–B and Ni–P amorphous alloy and its correlation to their catalytic properties," *Applied Surface Science*, vol. 152, no. 1-2, pp. 25–34, 1999.

[49] H. Li, H. X. Li, W. J. Wang, J. F. Deng, and J. F., "Excellent activity of ultrafine Co–B amorphous alloy catalyst in glucose hydrogenation," *Chemistry Letters*, no. 7, pp. 629–630, 1999.

[50] H. X. Li, H. S. Luo, L. Zhuang, W. L. Dai, and M. H. Qiao, "Liquid phase hydrogenation of furfural to furfuryl alcohol over the Fe-promoted Ni–B amorphous alloy catalysts," *Journal of Molecular Catalysis A*, vol. 203, no. 1-2, pp. 267–275, 2003.

[51] H. X. Li, H. Li, W. L. Dai, and M. H. Qiao, "Preparation of the Ni–B amorphous alloys with variable boron content and its correlation to the hydrogenation activity," *Applied Catalysis A*, vol. 238, no. 1, pp. 119–130, 2003.

[52] H. X. Li, Y. D. Wu, J. Zhang, W. L. Dai, and M. H. Qiao, "Liquid phase acetonitrile hydrogenation to ethylamine over a highly active and selective Ni–Co–B amorphous alloy catalyst," *Applied Catalysis A*, vol. 275, no. 1-2, pp. 199–206, 2004.

[53] H. Li, J. Zhang, and H. X. Li, "Ultrasound-assisted preparation of a novel Ni–B amorphous catalyst in uniform nanoparticles

for *p*-chloronitrobenzene hydrogenation," *Catalysis Communications*, vol. 8, no. 12, pp. 2211–2216, 2007.

[54] L. H. Lu, Y. H. Ma, F. Guo et al., "Structural characteristics of Mo modified skeletal Ni and its catalysis for liquid phase hydrogenation of nitro T-acid to T-acid," *Fine Chemicals*, vol. 25, no. 3, pp. 251–255, 2008.

[55] Y. F. Ma, W. Li, M. G. Zhang, Y. Zhou, and K. Y. Tao, "Preparation and catalytic properties of amorphous alloys in hydrogenation of sulfolene," *Applied Catalysis A*, vol. 246, no. 2, pp. 215–223, 2003.

[56] F. Cardenas-Lizana, S. Gomez-Quero, and M. A. Keane, "Clean production of chloroanilines by selective gas phase hydrogenation over supported Ni catalysts," *Applied Catalysis A*, vol. 334, no. 1-2, pp. 199–206, 2008.

[57] X. X. Han, R. X. Zhou, X. M. Zheng, and H. Jiang, "Effect of rare earths on the hydrogenation properties of *p*-chloronitrobenzene over polymer-anchored platinum catalysts," *Journal of Molecular Catalysis A*, vol. 193, no. 1-2, pp. 103–108, 2003.

[58] X. X. Han, R. X. Zhou, G. H. Lai, and X. M. Zheng, "Influence of support and transition metal (Cr, Mn, Fe, Co, Ni and Cu) on the hydrogenation of *p*-chloronitrobenzene over supported platinum catalysts," *Catalysis Today*, vol. 93–95, pp. 433–437, 2004.

[59] R. Hara, K. Sato, W. H. Sun, and T. Takahashi, "Catalytic dechlorination of aromatic chlorides using Grignard reagents in the presence of $(C_5H_5)_2TiCl_2$," *Chemical Communications*, vol. 12, no. 9, pp. 845–846, 1999.

[60] M. L. Hitchman, R. A. Spackman, N. C. Ross, and C. Agra, "Disposal methods for chlorinated aromatic waste," *Chemical Society Reviews*, vol. 24, no. 6, pp. 423–430, 1995.

[61] Y. J. Hou, Y. Q. Wang, F. He et al., "Liquid phase hydrogenation of 2-ethylanthraquinone over La-doped Ni–B amorphous alloy catalysts," *Materials Letters*, vol. 58, no. 7-8, pp. 1267–1271, 2004.

[62] G. Junfeng, A. J. David, and G. G. J. Brian, "Exploring the structural complexities of metal-metalloid nanoparticles: the case of Ni · B as catalyst," *Chemistry*, vol. 15, no. 5, pp. 1134–1143, 2009.

[63] V. Kratky, M. Kralik, M. Mecarova, M. Stolcova, L. Zalibera, and M. Hronec, "Effect of catalyst and substituents on the hydrogenation of chloronitrobenzenes," *Applied Catalysis A*, vol. 235, no. 1-2, pp. 225–231, 2002.

[64] I. H. Liu, C. Y. Chang, S. C. Liu, I. C. Chang, and S. M. Shih, "Absorption removal of sulfur dioxide by falling water droplets in the presence of inert solid particles," *Atmospheric Environment*, vol. 28, no. 21, pp. 3409–3415, 1994.

[65] Z. B. Yu, M. H. Qiao, H. X. Li, and J. F. Deng, "Preparation of amorphous Ni–Co–B alloys and the effect of cobalt on their hydrogenation activity," *Applied Catalysis A*, vol. 163, no. 1-2, pp. 1–13, 1997.

[66] H. Yamashita, H. Yoshikawa, T. Funabiki, and S. Yoshida, "Catalysis by amorphous metal alloys, part 4: structural modification towards metastable states and catalytic activity of amorphous $NI_{62}B_{38}$ ribbon alloy," *Journal of the Chemical Society, Faraday Transactions I*, vol. 82, no. 6, pp. 1771–1780, 1986.

[67] X. Yan, M. Liu, H. Liu, and K. Y. Liew, "Role of boron species in the hydrogenation of *o*-chloronitrobenzene over polymer-stabilized ruthenium colloidal catalysts," *Journal of Molecular Catalysis A*, vol. 169, no. 1-2, pp. 225–233, 2001.

[68] X. H. Yan, J. Q. Sun, Y. W. Wang, and J. F. Yang, "A Fe-promoted Ni–P amorphous alloy catalyst (Ni–Fe–P) for liquid phase hydrogenation of *m*- and *p*-chloronitrobenzene," *Journal of Molecular Catalysis A*, vol. 252, no. 1-2, pp. 17–22, 2006.

[69] X. H. Yan, J. Q. Sun, Y. H. Xu, and J. F. Yang, "Liquid-phase hydrogenation of chloronitrobenzene to chloroaniline over Ni–Co–B amorphous alloy catalyst," *Chinese Journal of Catalysis*, vol. 27, no. 2, pp. 119–123, 2006.

[70] J. Chen, N. Yao, R. Wang, and J. Zhang, "Hydrogenation of chloronitrobenzene to chloroaniline over Ni/TiO_2 catalysts prepared by sol-gel method," *Chemical Engineering Journal*, vol. 148, pp. 164–172, 2009.

[71] B. Coq, A. Tijani, and F. Figuéras, "Influence of alloying platinum for the hydrogenation of *p*-chloronitrobenzene over PtM/Al_2O_3 catalysts with M = Sn, Pb, Ge, Al, Zn," *Journal of Molecular Catalysis*, vol. 71, no. 3, pp. 317–333, 1992.

[72] B. Coq, A. Tijani, R. Dutartre, and F. Figueras, "Influence of support and metallic precursor on the hydrogenation of *p*-chloronitrobenzene over supported platinum catalysts," *Journal of Molecular Catalysis*, vol. 79, no. 1-3, pp. 253–264, 1993.

[73] M. G. Wang, H. X. Li, Y. D. Wu, and J. Zhang, "Comparative studies on the catalytic behaviors between the Ni–B amorphous alloy and other Ni-based catalysts during liquid phase hydrogenation of acetonitrile to ethylamine," *Materials Letters*, vol. 57, no. 19, pp. 2954–2964, 2003.

[74] C. A. Tolman, W. H. Riggs, W. J. Lin, C. M. King, and R. C. Wendt, "Electron spectroscopy for chemical analysis of nickel compounds," *Inorganic Chemistry*, vol. 12, no. 12, pp. 2770–2778, 1973.

[75] L. J. Matienzo, L. I. Yin, S. O. Grim, and W. E. Swartz Jr., "X-ray photoelectron spectroscopy of nickel compounds," *Inorganic Chemistry*, vol. 12, no. 12, pp. 2762–2769, 1973.

[76] W. L. Dai, M. H. Qiao, and J. F. Deng, "XPS studies on a novel amorphous Ni–Co–W–B alloy powder," *Applied Surface Science*, vol. 120, no. 1-2, pp. 119–124, 1997.

[77] J. F. Moulder, W. F. Stickle, P. E. Sobol, and K. D. Bomben, *Handbook of X-Ray Photoelectron Spectroscopy*, Physical Electronics, Chanhassen, Minn, USA, 1995.

[78] J. Tamaki, S. Nakayama, M. Yamamura, and T. Imanaka, "Preparation and catalytic properties of palladium-(boron, phosphorus) thin films using an RF sputtering method," *Journal of Materials Science*, vol. 24, no. 5, pp. 1582–1588, 1989.

[79] J. H. Shen and Y. W. Chen, "Catalytic properties of bimetallic NiCoB nanoalloy catalysts for hydrogenation of *p*-chloronitrobenzene," *Journal of Molecular Catalysis A*, vol. 273, no. 1-2, pp. 265–276, 2007.

[80] H. Noller and W. M. Lin, "Activity and selectivity of $Ni = Cu/Al_2O_3$ catalysts for hydrogenation of crotonaldehyde and mechanism of hydrogenation," *Journal of Catalysis*, vol. 85, no. 1, pp. 25–30, 1984.

[81] O. Levenspiel, *Chemical Reaction Engineering*, John Wiley & Sons, New York, NY, USA, 1999.